AD-A189 414 PHASE VELOCITY AND ATTENUATION OF PLANE ELASTIC WAVES 1/1
IN A PARTICLE-REINF (U) COLORADO UNIV AT BOULDER DEPT
OF MECHANICAL ENGINEERING S K DATTA ET AL AUG 87

UNCLASSIFIED CUMER-87-3 N00014-86-K-0280 F/G 11/4 NL

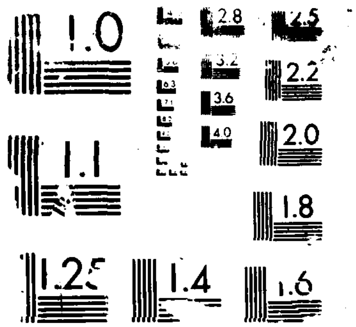
1.0
2.8
2.5
3.2
2.2
3.6
4.0
2.0
1.1
1.8
1.25
1.4
1.6

Contract N00014-86-K-0280

PHASE VELOCITY AND ATTENUATION OF PLANE ELASTIC WAVES IN A PARTICLE-REINFORCED COMPOSITE MEDIUM

S.K. Datta
University of Colorado, CIRES
H.M. Ledbetter
National Bureau of Standards
Y. Shindo
Tohoku University
A.H. Shah
University of Manitoba

CUMER 87-3 August, 1987

PHASE VELOCITY AND ATTENUATION OF PLANE ELASTIC WAVES IN A PARTICLE-REINFORCED COMPOSITE MEDIUM

S.K. Datta
Department of Mechanical Engineering and CIRES, University of Colorado, Boulder, Colorado 80309, U.S.A.

H.M. Ledbetter
Fracture and Deformation Division, Institute for Materials Science and Engineering, NBS, Boulder, Colorado 80303, U.S.A.

Y. Shindo
Department of Mechanical Engineering, Tohoku University, Sendai 980, Japan

A.H. Shah
Department of Civil Engineering, University of Manitoba, Winnipeg R3T2N2, Canada

Received _________, Revised ________.

Lead Silicon Carbide/Aluminum

Our study considered effective-plane-wave propagation, both longitudinal and shear, through a medium containing a random distribution of spherical inclusions. We assumed that the particles and matrix are separated by a thin layer of elastic material with different properties. For some systems, we predict measurable effects for the thin layers. Especially, we considered Pb/epoxy and SiC/Al.

1. Introduction

Wave propagation through a particle-reinforced composite medium has been studied by many authors [1-13]. Except [5], all these studies assume that the inclusions bond perfectly with the surrounding matrix material. In [5], for long wavelengths, the authors consider the effect of a thin viscous third layer. Recently, Sayers [11] examined the effect of this layer when the particles and the matrix possess the same properties.

In the present study, we analyze the problem of wave propagation in a composite medium with a random distribution of spherical inclusions. The inclusions are separated from the matrix by thin layers of elastic material. The properties of the layers vary through the thickness such that there is a continuous transition from the inclusions to the matrix.

The object of this study was to explore the practicality of using ultrasound to characterize properties of interface layers. Ultrasound is a practical tool for measuring properties of, and characterizing the state of, a material with microstructure (or changes in microstructure). References to such studies occur in ~~[11]~~

2. Scattering by a spherical inclusion with an interface layer

Consider a spherical inclusion of radius a and elastic properties λ_1, μ_1, ρ_1 embedded in an elastic matrix of material properties λ_2, μ_2, ρ_2. Also, let the inclusion be separated from the matrix by a thin layer of uniform thickness h(<<a) with variable material properties $\lambda(r)$, $\mu(r)$, and $\rho(r)$. Here, λ, μ denote Lamé constants and ρ density. Let $\lambda(r)$, $\mu(r)$ be expressed as

$$\lambda(r) + 2\mu(r) = (\lambda_1 + 2\mu_1)f(r), \quad a < r < a + h, \tag{1}$$

$$\mu(r) = \mu_1 g(r), \quad a < r < a + h. \tag{2}$$

Here, f(r) and g(r) denote general functions of r. A special case arises when

$$f(a) = 1, \quad g(a) = 1,$$

$$f(a + h) = \frac{\lambda_2 + 2\mu_2}{\lambda_1 + 2\mu_1}, \quad g(a + h) = \frac{\mu_2}{\mu_1}, \tag{3}$$

with the stipulation that f(r) and g(r) with their first derivatives are continuous in (a, a + h). Since h is assumed to be much smaller than a, it follows from (3) that f'(a) and g'(a) can be approximated by

$$f'(a) = \frac{(\lambda_2 + 2\mu_2) - (\lambda_1 + 2\mu_1)}{h(\lambda_1 + 2\mu_1)},$$

$$g'(a) = \frac{\mu_2 - \mu_1}{h\mu_1}. \tag{4}$$

Another special case arises when the interface material possesses constant properties. Then we have

$$f(r) = (\lambda_i' + 2\mu_i')/(\lambda_1 + 2\mu_1), \quad g(r) = \mu_i'/\mu_1. \tag{5}$$

Here λ_i', μ_i' are the Lamé constants for the interface material.

We also make the assumption that h is much smaller than the wavelength of the propagating wave. Then, to first order in h/λ, λ being the wavelength,

$$\tau_{rr}^{t} = \tau_{rr}^{s} + \tau_{rr}^{i}, \quad \tau_{r\theta}^{t} = \tau_{r\theta}^{s} + \tau_{r\theta}^{i},$$

$$\tau_{r\Phi}^{t} = \tau_{r\Phi}^{s} + \tau_{r\Phi}^{i}. \tag{6}$$

Here τ_{ij} is the stress tensor and superscripts t, s, and i denote the transmitted, scattered, and incident field quantities, respectively. Note that τ_{ij}^{s}, τ_{ij}^{i}, and τ_{ij}^{t} appearing above are calculated at $r = a$. The spherical polar coordinates r, θ, Φ are defined in Fig. 1. Boundary conditions (6) express the fact that, to first order in h/λ, the traction components do not suffer any jump across the layer. However, the displacement components suffer jumps given by

$$u_r^s + u_r^i - u_r^t = \frac{hK_1}{\lambda_1 + 2\mu_1} \tau_{rr}^{t}, \tag{7}$$

$$u_\theta^s + u_\theta^i - u_\theta^t = \frac{hK_2}{\mu_1} \tau_{r\theta}^{t}, \tag{8}$$

$$u_\Phi^s + u_\Phi^i - u_\Phi^t = \frac{hK_2}{\mu_1} \tau_{r\Phi}^{t}. \tag{9}$$

Here,

$$K_1 = \int_0^1 \frac{dx}{f(a + hx)}, \quad K_2 = \int_0^1 \frac{dx}{g(a + hx)}. \tag{10}$$

Using equations (3) and (4) in (10), we find that K_1 and K_2 are given approximately by

$$K_1 = \frac{\lambda_1 + 2\mu_1}{\lambda_2 + 2\mu_2 - (\lambda_1 + 2\mu_1)} \ln \left[1 + \frac{\lambda_2 + 2\mu_2 - (\lambda_1 + 2\mu_1)}{\lambda_1 + 2\mu_1}\right], \tag{11}$$

$$K_2 = \frac{\mu_1}{\mu_2 - \mu_1} \ln \left[1 + \frac{\mu_2 - \mu_1}{\mu_1}\right]. \tag{12}$$

On the other hand, if eq. (5) is used, then

$$K_1 = (\lambda_1 + 2\mu_1)/(\lambda_1' + 2\mu_1'),\ K_2 = \mu_1/\mu_1'. \tag{13}$$

Mal and Bose [5] studied a problem similar to the one considered here. They assumed a thin viscous third layer between the sphere and the matrix and imposed the condition of radial-displacement continuity.

We assumed the incident wave to be either a plane longitudinal wave propagating in the positive z-direction or a plane shear wave polarized in the x-direction and propagating in the positive z-direction. Thus,

$$\underset{\sim}{u}^i = e^{ik_1 z}\underset{\sim}{e}_z + e^{ik_2 z}\underset{\sim}{e}_x. \tag{14}$$

Here, $k_1 = \omega/c_1$ and $k_2 = \omega/c_2$. ω denotes the circular frequency of the wave and c_1, c_2 denote the longitudinal and shear wave speeds in the matrix. The factor $e^{-i\omega t}$ was suppressed.

$\underset{\sim}{u}^i$ given above can be expanded in spherical vector wave functions as

$$\underset{\sim}{u}^i = \frac{1}{ik_1} \sum_{n=0}^{\infty} i^n (2n + 1) \underset{\sim}{L}^{(1)}_{on}$$

$$+ \frac{1}{2i} \sum_{n=1}^{\infty} \sum_{m=-1}^{1} \frac{2n + 1}{n(n + 1)} i^n \left[\underset{\sim}{M}^{(1)}_{mn}(\delta_{m1} + n(n + 1)\ \delta_{m,-1})\right.$$

$$\left. + \frac{1}{k_2} \underset{\sim}{N}^{(1)}_{mn}(\delta_{m1} - n(n + 1)\ \delta_{m,-1})\right]. \tag{15}$$

Vector wave functions $\underset{\sim}{L}^{(1)}$, $\underset{\sim}{M}^{(1)}$ and $\underset{\sim}{N}^{(1)}$ appearing above are regular at r = 0 and are given by

$$\underset{\sim}{L}^{(1)}_{mn} = \Big[\underset{\sim}{e}_r \frac{\partial}{\partial r} j_n (k_1 r)\ P^m_n (\cos\theta) + \underset{\sim}{e}_\theta\ j_n (k_1 r) \frac{1}{r}\frac{\partial}{\partial\theta} P^m_n (\cos\theta)$$

$$+ \underset{\sim}{e}_\Phi \frac{im}{r\sin\theta} j_n (k_1 r)\ P^m_n (\cos\theta)\Big]\ e^{im\Phi}\ ,$$

$$\underset{\sim}{M}_{mn} = \Big[\underset{\sim}{e}_\theta \frac{im}{\sin\theta} j_n (k_2 r)\ P^m_n (\cos\theta) - \underset{\sim}{e}_\Phi\ j_n (k_2 r) \frac{\partial}{\partial\theta} P^m_n (\cos\theta)\Big]\ e^{im\Phi}\ ,$$

$$\underset{\sim}{N}^{(1)}_{mn} = \Big[\underset{\sim}{e}_r \frac{n(n+1)}{r} j_n (k_2 r)\ P^m_n (\cos\theta) + \underset{\sim}{e}_\theta \frac{1}{r}\frac{\partial}{\partial r} (r j_n\ k_2 r))x$$

$$\frac{\partial}{\partial\theta} P^m_n (\cos\theta) + \underset{\sim}{e}_\Phi \frac{im}{r\sin\theta}\frac{\partial}{\partial r} (r j_n(k_2 r))\ P^m_n (\cos\theta)\Big]\ \underset{\sim}{e}^{im\Phi}\ . \tag{16}$$

The scattered and transmitted fields can be written

$$\underset{\sim}{u}^s = \sum_{n=0}^{\infty} \sum_{m=-1}^{1} [A_{mn}\ \underset{\sim}{L}^{(3)}_{mn}\ \delta_{mo} + B_{mn}\ \underset{\sim}{M}^{(3)}_{mn} + C_{mn}\ \underset{\sim}{N}^{(3)}_{mn}]\ , \tag{17}$$

$$\underset{\sim}{u}^t = \sum_{n=0}^{\infty} \sum_{m=-1}^{1} [A'_{mn}\ \underset{\sim}{L}^{(1)\prime}_{mn}\ \delta_{mo} + B'_{mn}\ \underset{\sim}{M}^{(1)\prime}_{mn} + C'_{mn}\ \underset{\sim}{N}^{(1)\prime}_{mn}]\ . \tag{18}$$

Here, the prime denotes that k_1 and k_2 are to be replaced by k_1' ($= \omega/c_1'$) and k_2' ($= \omega/c_2'$), respectively. c_1' and c_2' are the wave speeds in the inclusion. $\underset{\sim}{L}^{(3)}$, $\underset{\sim}{M}^{(3)}$, and $\underset{\sim}{N}^{(3)}$ are obtained by replacing j_n by h_n in (16). Note that j_n is the spherical Bessel function of the first kind, and h_n is the spherical Hankel function of the first kind.

The constants A, B, C, A', B', C' are found by using conditions (7) and (8)-(10). For this purpose, we define the following matrices:

$$M_n = \begin{bmatrix} F_n & G_n \\ H_n & I_n \end{bmatrix}, \tag{19}$$

$$L_n = \begin{bmatrix} SF_n & SG_n \\ SH_n & SI_n \end{bmatrix}. \tag{20}$$

Here,

$$F_n(k_1 a) = nh_n(k_1 a) - k_1 a h_{n+1}(k_1 a),$$
$$G_n(k_2 a) = n(n+1)\, h_n(k_2 a),\ H_n(k_1 a) = h_n(k_1 a),$$
$$I_n(k_2 a) = (n+1)\, h_n(k_2 a) - k_2 a h_{n+1}(k_2 a),$$
$$SF_n(k_1 a) = (n^2 - n - \tfrac{1}{2} k_2^2 a^2)\, h_n(k_1 a) + 2k_1 a h_{n+1}(k_1 a),$$
$$SG_n(k_2 a) = n(n+1)\, [(n-1)\, h_n(k_2 a) - k_2 a h_{n+1}(k_2 a)],$$
$$SH_n(k_1 a) = (n-1)\, h_n(k_1 a) - k_1 a h_{n+1}(k_1 a),$$
$$SI_n(k_2 a) = (n^2 - 1 - \tfrac{1}{2} k_2^2 a^2)\, h_n(k_2 a) + k_2 a h_{n+1}(k_2 a).$$

Equations to determine A_{mn} and B_{mn} are found to be

$$\left[\frac{2h}{a}\kappa\, L_n - M_n + \frac{\mu_2}{\mu_1} M'_n\, L'^{-1}_n\, L_n\right] \begin{Bmatrix} A_{mn} \\ C_{mn} \end{Bmatrix} =$$

$$a \begin{Bmatrix} u^{i}_{r(mn)} \\ u^{1i}_{\theta(mn)} \end{Bmatrix} - \frac{a^2}{2\mu_2} \left[\frac{2h}{a}\kappa + \frac{\mu_2}{\mu_1} M'_n\, L'^{-1}_n\right] \begin{Bmatrix} \tau^{i}_{rr(mn)} \\ \tau^{1i}_{r\theta(mn)} \end{Bmatrix}. \tag{21}$$

Here

$$\kappa = \begin{bmatrix} \dfrac{\mu_2}{\lambda_1 + 2\mu_1} K_1 & 0 \\ 0 & \dfrac{\mu_2}{\mu_1} K_2 \end{bmatrix}.$$

M_n', L_n' are obtained from M_n, L_n, respectively, by replacing h_n and h_{n+1} by j_n and j_{n+1}, respectively, in (19) and (20), and by replacing k_1 and k_2 by k_1' and k_2', respectively. In writing (21) we express u_r^i and u_θ^i given by (15) as

$$u_r^i = \sum_{n=0}^{\infty} \sum_{m=-1}^{1} u_{r(mn)}^i \, P_n^m (\cos\theta) e^{im\Phi} ,$$

$$u_\theta^i = \sum_{n=0}^{\infty} \sum_{m=-1}^{1} \left\{ u_{\theta(mn)}^{1i} \frac{\partial P_n^m}{\partial\theta} + u_{\theta(mn)}^{2i} \frac{im}{\sin\theta} P_n^m \right\} e^{im\Phi} . \tag{22}$$

It then follows that

$$\begin{Bmatrix} \tau_{rr(mn)}^i \\ \tau_{r\theta(mn)}^{1i} \end{Bmatrix} = \frac{2\mu_2}{a} \bar{L}_n \bar{M}_n^{-1} \begin{Bmatrix} u_{r(mn)}^i \\ u_{\theta(mn)}^{1i} \end{Bmatrix} . \tag{23}$$

$\bar{L}_n$ and $\bar{M}_n$ are obtained from L_n and M_n respectively, by replacing h_n and h_{n+1} by j_n and j_{n+1}, respectively.

The equation to find B_{mn} is

$$\left[\frac{h}{a} \kappa_{22} \, ((n-1) \, h_n(k_2a) - k_2ah_{n+1}(k_2a)) - \right.$$

$$\left. h_n(k_2a) + \frac{\mu_2}{\mu_1} j_n(k_2'a) \frac{(n-1) \, h_n(k_2a) - k_2ah_{n+1}(k_2a)}{(n-1) \, j_n(k_2'a) - k_2'aj_{n+1}(k_2'a)}\right] B_{mn} \tag{24}$$

$$= u_{\theta(mn)}^{2i} - \frac{a}{\mu_2} \left[\frac{h}{a} \kappa_{22} + \frac{\mu_2}{\mu_1} \frac{j_n(k_2'a)}{(n-1) \, j_n(k_2'a) - k_2'aj_{n+1}(k_2'a)}\right] \tau_{r\theta(mn)}^{2i}$$

Here,

$$\tau_{r\theta(mn)}^{2i} = \frac{\mu_2}{a} \frac{(n-1) \, j_n(k_2a) - k_2aj_{n+1}(k_2a)}{j_n(k_2a)} \, u_{\theta(mn)}^{2i} . \tag{25}$$

Once A_{mn}, C_{mn}, and B_{mn} are determined by solving (21) and (24), the scattered field is then found from (17). Since the expressions for the field inside the inclusion will not be needed to derive the dispersion equation governing the effective wavenumber of plane-wave propagation through the composite medium, we omit these.

3. Distribution of inclusions

In [5, 14] the scattered-field expressions were used to calculate effective wave speeds at long wavelengths in a medium with a distribution of spherical inclusions with interface layers. A 'quasicrystalline' approximation together with the assumption of no correlation was used to derive expressions for the effective wave speeds. As has been shown [12], particular forms of two-particle correlations can be included in the formalism. But this leads to complicated equations that require numerical solutions.

In this study, we adopt the approach taken in [10, 11] to calculate approximate phase velocities and attenuation of plane-longitudinal and plane-shear waves. In this simple approximation, the effective wavenumber k is related to the forward scattered amplitude by the equation [15]:

$$K^2 = k_0^2 + 4\pi n\bar{f}(K) \quad . \tag{26}$$

Here, k_0 is the wavenumber in the absence of scatterers, n the number density of scatterers, and $\bar{f}$ the averaged forward-scattered amplitude. Equation (26) is an implicit equation for the determination of the (complex) wavenumber K. A further simplification occurs when the solution to (26) is taken as

$$K^2 = k_0^2 + 4\pi n_0\bar{f}(k_0) . \tag{27}$$

Equation (27) was derived by Foldy [16] and has been used by many authors to calculate the frequency dependence of phase velocity and attenuation of plane waves. Equations (26) and (27) are valid for low volume concentrations of inclusions.

Using (17) in (26), we find that for longitudinal waves the effective wave number is

$$\left(\frac{K_1}{k_1}\right)^2 = 1 + \frac{4\pi n_0}{k_1^2} \sum_{n=0}^{\infty} (-i)^n A_{on}(K_1, K_2). \tag{28}$$

For shear waves we obtain

$$\left(\frac{K_2}{k_2}\right)^2 = 1 + \frac{4\pi n_0}{k_2^2} \sum_{n=1}^{\infty} (-i)^n \tfrac{1}{2} n(n+1) \left(C_{1n} + k_2^{-1} B_{1n} - \frac{1}{n(n+1)} (C_{-1n} - k_2^{-1} B_{-1n})\right). \tag{29}$$

In the following section we present phase velocity and attenuation calculated from the above two equations. Note that the real part of K/k gives the velocity ratio c/C, where c is the velocity in the matrix and C is the effective velocity in the composite. The attenuation of power is obtained from the equation

$$\frac{\alpha}{k} = 2 \operatorname{Im} \frac{K}{k}. \tag{30}$$

For dilute concentration this equation reduces to

$$\frac{\alpha}{k} = n_0 \Sigma. \tag{31}$$

Here, Σ denotes scattering cross section.

4. Numerical results and discussion

Computations were made for two particular composite materials: lead-epoxy and SiC-Al. For both materials, we consider two interface thicknesses: zero and 0.1a, through which the properties vary linearly from the inclusion to the matrix.

Numerical results for the lead-epoxy composite based on a simplified eq. (27) were presented in [10]. Figures 2 and 3 show the attenuation and phase velocity of a longitudinal wave when the interface thickness equals zero. These results agree with those given in [10]. Also shown in these figures are the results for $h/a = 0.1$. It is seen that this thickness has little effect. At intermediate frequencies, the interface lowers the phase velocity and slightly increases the attenuation. Figures 4 and 5 show the results for the shear wave; the effect is slightly larger at moderate frequencies. We also computed the phase velocity and attenuation using eq. (26). Figure 6 shows that eq. (27) overestimates the attenuation. For phase velocity, however, as shown in Fig. 7, eq. (26) overestimates it at low frequencies, underestimates it at moderate frequencies, and gives nearly the same results at high frequencies.

Finally, in Figures 8-11 we show results for the second example: SiC–Al. These results are based on eq. (27) and show that the interface decreases both the attenuation and the phase velocity.

5. Conclusions

We considered the effect of thin interface layers between the inclusions and the matrix in modifying the dynamic properties of composite materials. Dynamic effective properties were calculated by using Foldy's equations. We found that interface effects are larger in some composites. We also studied the predictions based on iterative solutions of modified Foldy's equations in which the scattering amplitudes were calculated assuming that the matrix had the properties of the composite. This iterative solution underestimates attenuation in general; at low frequencies it overestimates phase velocity.

6. Acknowledgment

This study was supported in part by a grant from the Office of Naval Research (N00014--86-K-0280; Program Manager: Dr. Y. Rajapakse). Partial support was also provided by National Science and Engineering Research Council of Canada (Grant #A-7988) and by the Office of Nondestructive Evaluation, NBS. This work was completed when S.K.D. held a Faculty Fellowship award from the University of Colorado and a Fulbright Research Award at the Technical University of Vienna.

References

[1] P.C. Waterman and R. Truell, "Multiple scattering of elastic waves", J. Math. Phys. 2, 512-537 (1961).

[2] N. Yamakawa, "Scattering and attenuation of elastic waves", Geophys. Mag. (Tokyo) 31, 97-103 (1962).

[3] J.G. Fikioris and P.C. Waterman, "Multiple Scattering of Waves, II.", J. Math. Phys. 5, 1413-1420 (1964).

[4] A.K. Mal and L. Knopoff, "Elastic wave velocities in two component systems", J. Inst. Math. Appl. 3, 376-387 (1967).

[5] A.K. Mal and S.K. Bose, "Dynamic elastic moduli of a suspension of imperfectly bonded spheres", Proc. Camb. Phil. Soc. 76. 587-600 (1974).

[6] G.T. Kuster and N. Toksöz, "Velocity and attenuation of seismic waves in two-phase media: Part I. Theoretical calculations", Geophys. 39, 587-606 (1974).

[7] S.K. Datta, "A self-consistent approach to multiple scattering of elastic waves", J. Appl. Mech. 44, 657-662 (1977).

[8] J.G. Berryman, "Long-wavelength propagation in composite elastic media I. Spherical inclusions", J. Acoust. Soc. Am. 68, 1809-1819 (1980).

[9] A.J. Devaney and H. Levine, "Effective elastic parameters of random composites", Appl. Phys. Lett. 37, 377-379 (1980).

[10] C.M. Sayers and R.L. Smith, "Ultrasonic velocity and attenuation in an epoxy matrix containing lead inclusions", J. Phys. D: Appl. Phys. 16, 1189-1194 (1983).

[11] C.M. Sayers, "Scattering of ultrasound by minority phases in polycrystalline metals", Wave Motion 7, 95-104 (1985).

[12] V.K. Varadan, Y. Ma, and V.V. Varavan, "A multiple scattering theory for elastic wave propagation in discrete random medium", J. Acoust. Soc. Am. 77, 375-385 (1985).

[13] H.M. Ledbetter and S.K. Datta, "Effective wave speeds in an SiC-particle-reinforced $A\ell$ composite", J. Acoust. Soc. Am. 79, 239-248 (1986).

[14] S.K. Datta and H.M. Ledbetter, "Effect of interface properties on wave propagation in a medium with inclusions", in: A.P.S. Selvadurai and G.Z. Voyiadjis, eds., Mechanics of Material Interfaces, Elsevier, Amsterdam (1986) 131-141.

[15] J.E. Gubernatis and E. Domany, "Effects of microstructure on the speed and attenuation of elastic waves in porous materials", Wave Motion 6, 579-589 (1984).

[16] L.L. Foldy, "Multiple scattering theory of waves", Phys. Rev. 67, 107-119 (1945).

Table 1.

Properties of constituents

	Density (g/cm^3)	E(GPa)	μ(GPa)
Lead	11.3	23.57	8.35
Epoxy	1.18	4.31	1.57
SiC	3.181	440.6	188.1
Al	2.706	71.6	26.7

List of Figures

Fig. 1. Geometry of a spherical inclusion with an interface layer.

Fig. 2. Attenuation of longitudinal waves in a lead-epoxy composite with and without interface layer.

Fig. 3. Phase velocity of longitudinal waves in a lead-epoxy composite with and without interface layer.

Fig. 4. Attenuation of shear waves in a lead-epoxy composite with and without interface layer.

Fig. 5. Phase velocity of shear waves in a lead-epoxy composite with and without interface layer.

Fig. 6. Comparison of attenuation coefficients for longitudinal waves in a lead-epoxy composite predicted by an iterative solution of eq. (26) and by eq. (27).

Fig. 7. Comparison of phase velocities of longitudinal waves in a lead-epoxy composite predicted by an iterative solution of eq. (26) and by eq. (27).

Fig. 8. Attenuation of longitudinal waves in an SiC-Al composite with and without interface layer.

Fig. 9. Phase velocity of longitudinal waves in an SiC-Al composite with and without interface layer.

Fig. 10. Attenuation of shear waves in an SiC/Al composite with and without interface layer.

Fig. 11. Phase velocity of shear waves in an SiC/Al composite with and without interface layer.

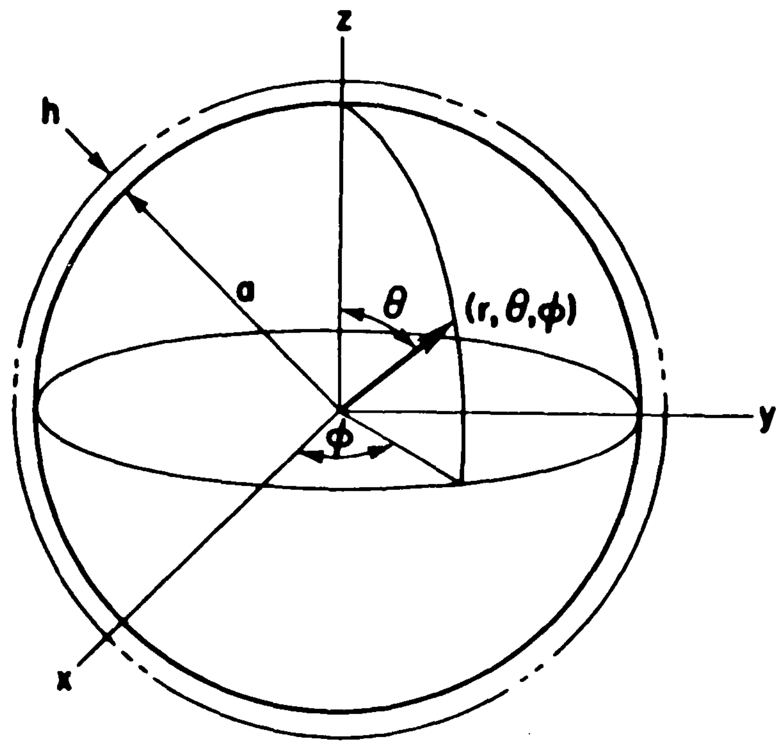
z
h
a
θ
(r, θ, φ)
y
φ
x

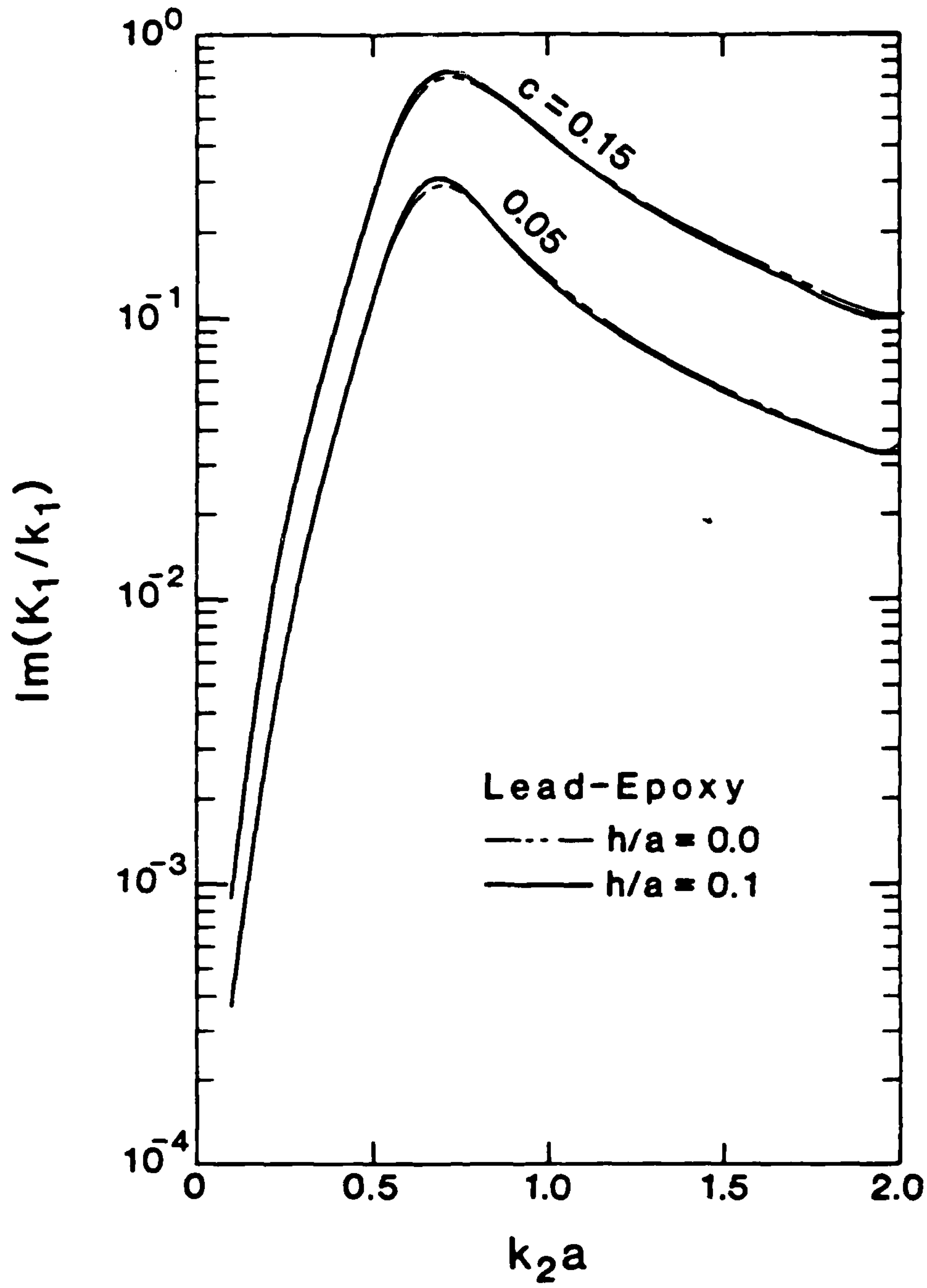

10^0
10^{-1}
10^{-2}
10^{-3}
10^{-4}
0
0.5
1.0
1.5
2.0
k_2a
$\mathrm{Im}(K_1/k_1)$
c = 0.15
0.05
Lead-Epoxy
h/a = 0.0
h/a = 0.1

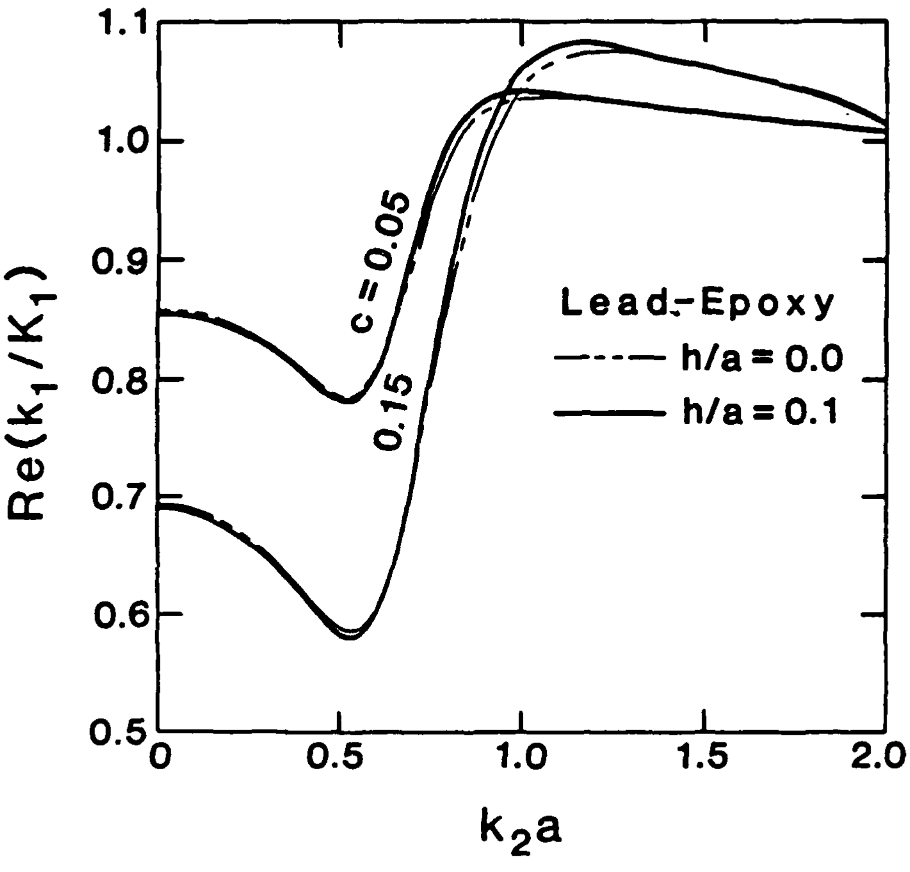

Re(k1/K1)
k2a
c=0.05
0.15
Lead-Epoxy
h/a=0.0
h/a=0.1

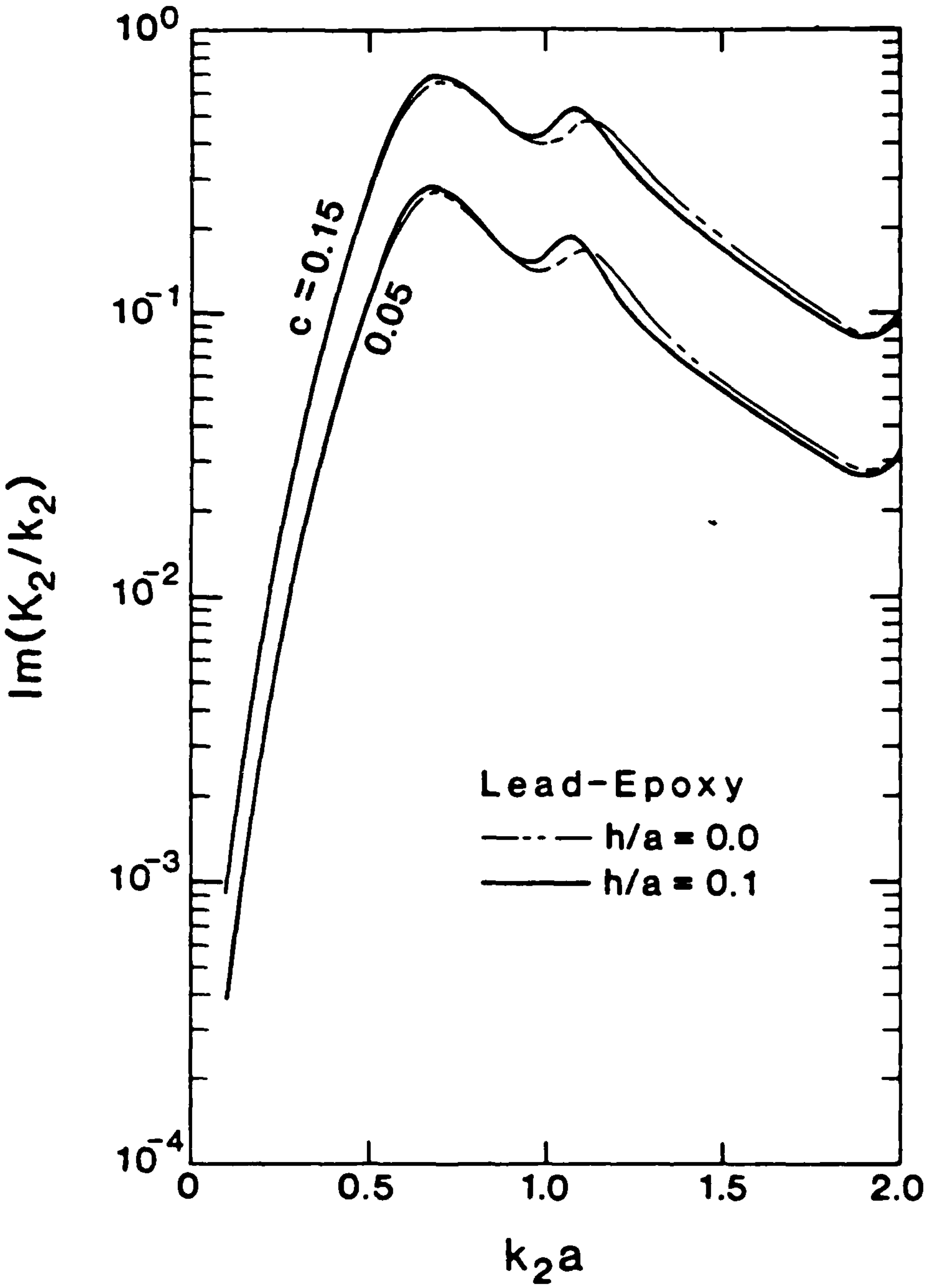

10^0
10^{-1}
10^{-2}
10^{-3}
10^{-4}
$\mathrm{Im}(K_2/k_2)$
c = 0.15
0.05
Lead-Epoxy
h/a = 0.0
h/a = 0.1
0
0.5
1.0
1.5
2.0
k_2a

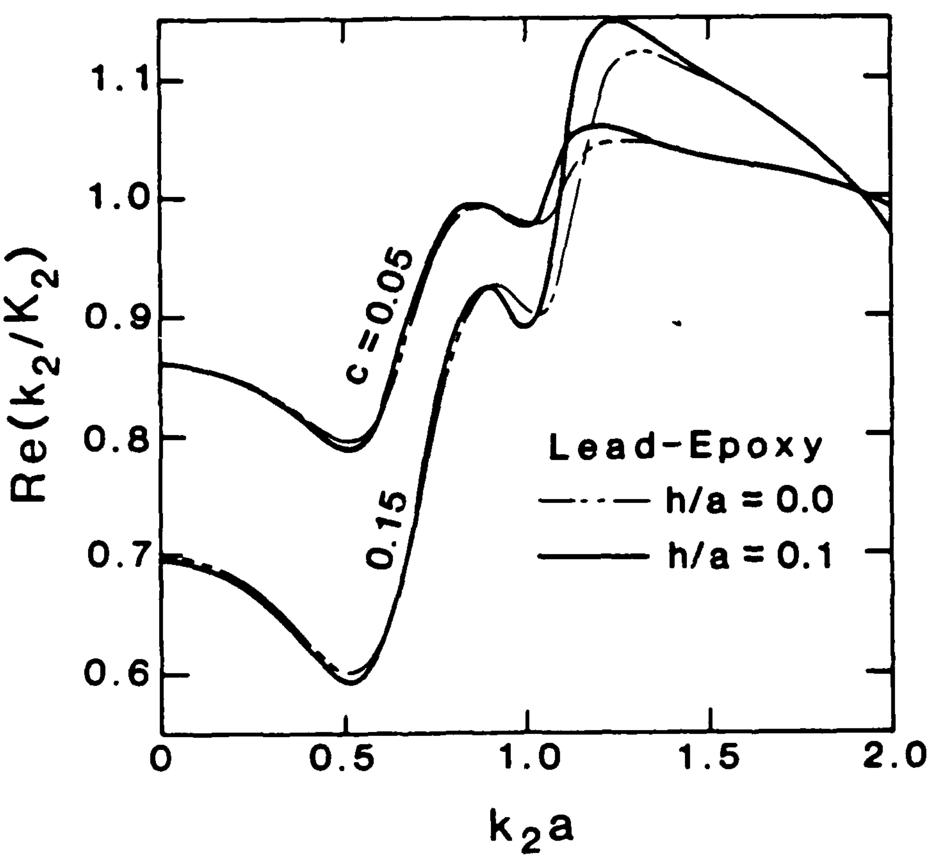

1.1
1.0
0.9
0.8
0.7
0.6
Re(k_2/K_2)
c = 0.05
0.15
Lead-Epoxy
h/a = 0.0
h/a = 0.1
0
0.5
1.0
1.5
2.0
k_2a

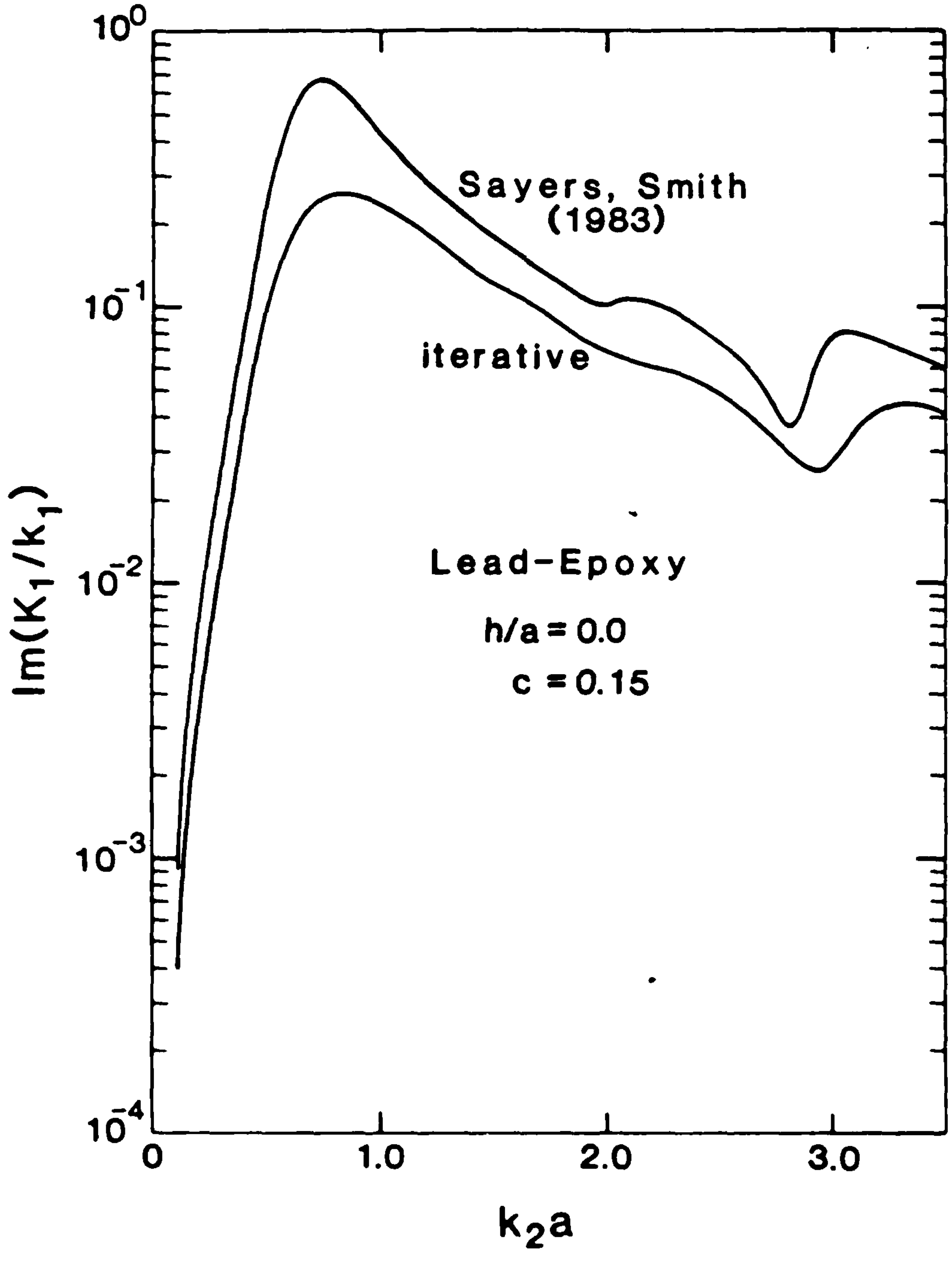

10^0
10^{-1}
10^{-2}
10^{-3}
10^{-4}
$\mathrm{Im}(K_1/k_1)$
0
1.0
2.0
3.0
k_2a
Sayers, Smith
(1983)
iterative
Lead-Epoxy
h/a = 0.0
c = 0.15

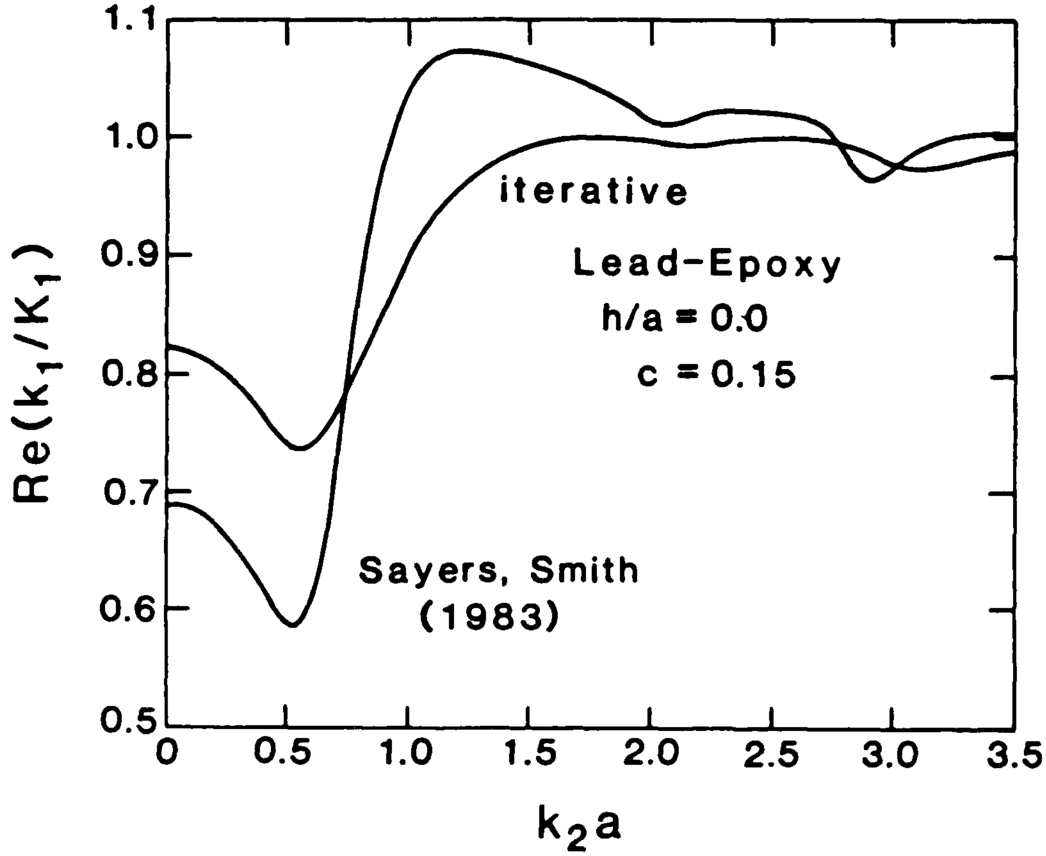

iterative
Lead-Epoxy
h/a = 0.0
c = 0.15
Sayers, Smith
(1983)
Re(k1/K1)
k2a
1.1
1.0
0.9
0.8
0.7
0.6
0.5
0
0.5
1.0
1.5
2.0
2.5
3.0
3.5

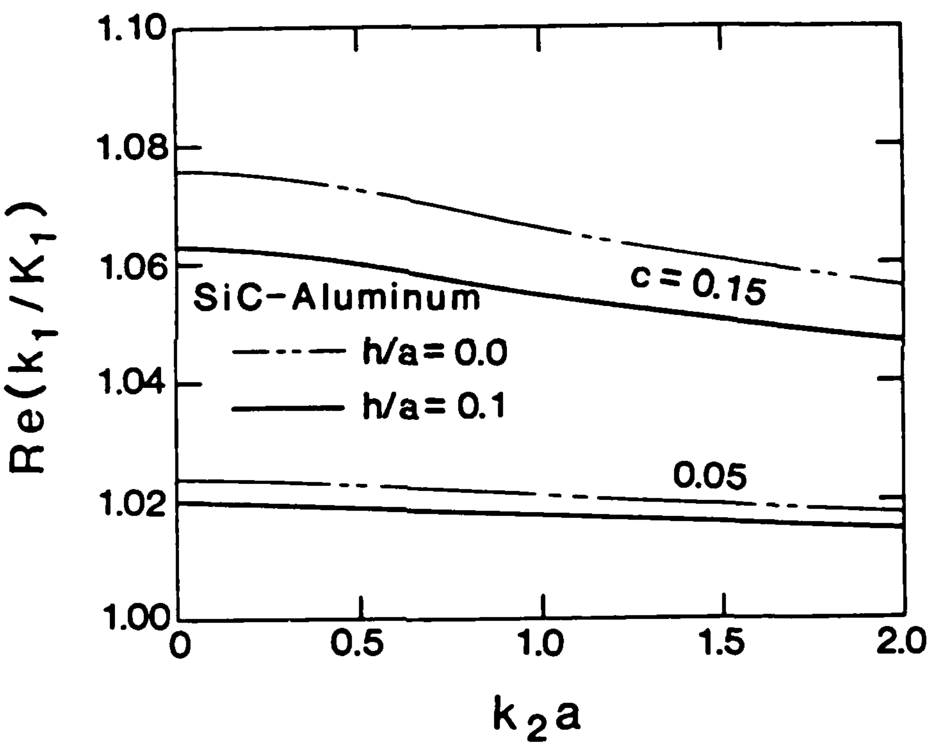

1.10
1.08
1.06
1.04
1.02
1.00
0
0.5
1.0
1.5
2.0
Re(k1/K1)
k2a
SiC-Aluminum
h/a= 0.0
h/a= 0.1
c = 0.15
0.05

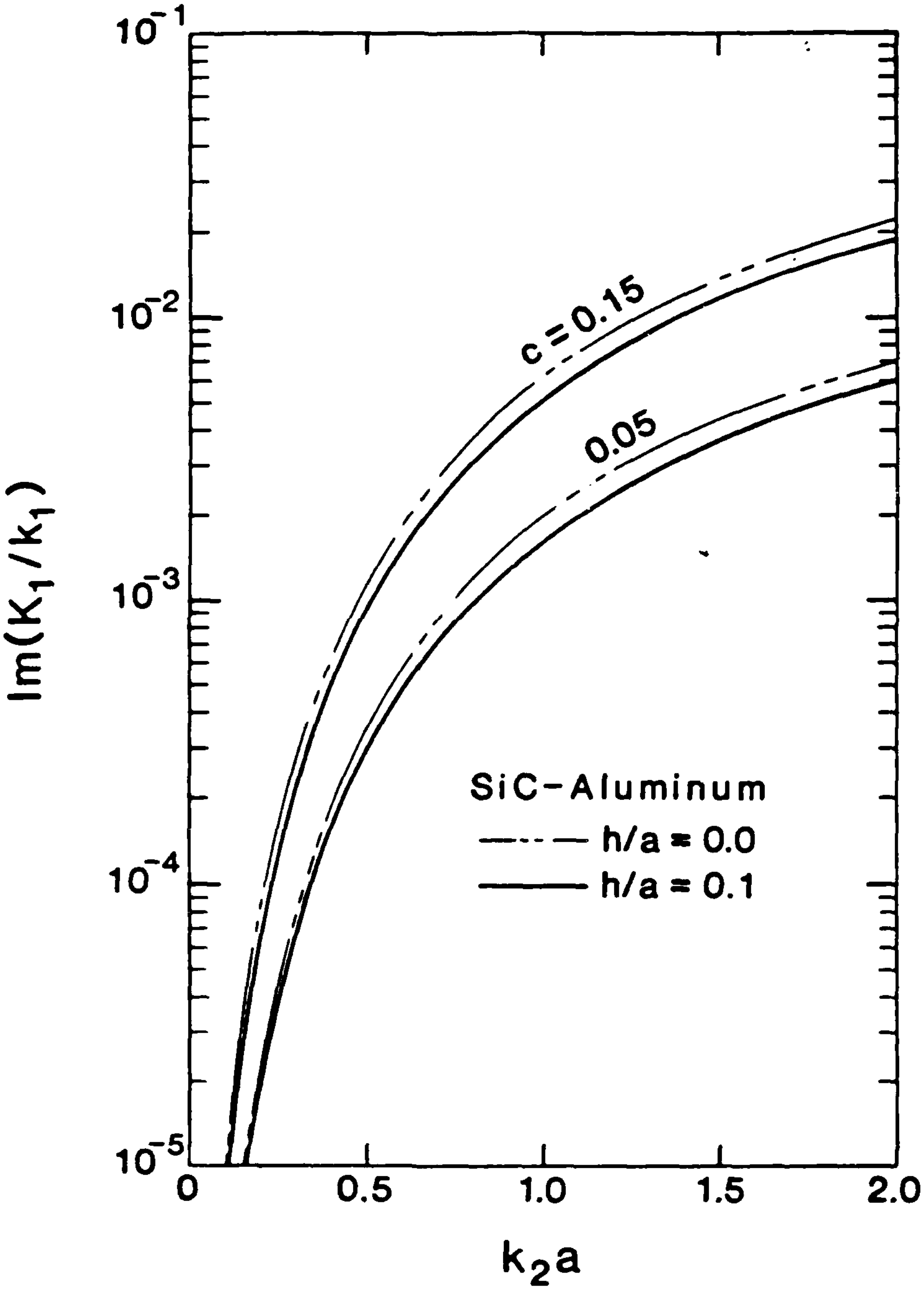

10^-1
10^-2
10^-3
10^-4
10^-5
Im(K1/k1)
c = 0.15
0.05
SiC-Aluminum
h/a = 0.0
h/a = 0.1
0
0.5
1.0
1.5
2.0
k2a

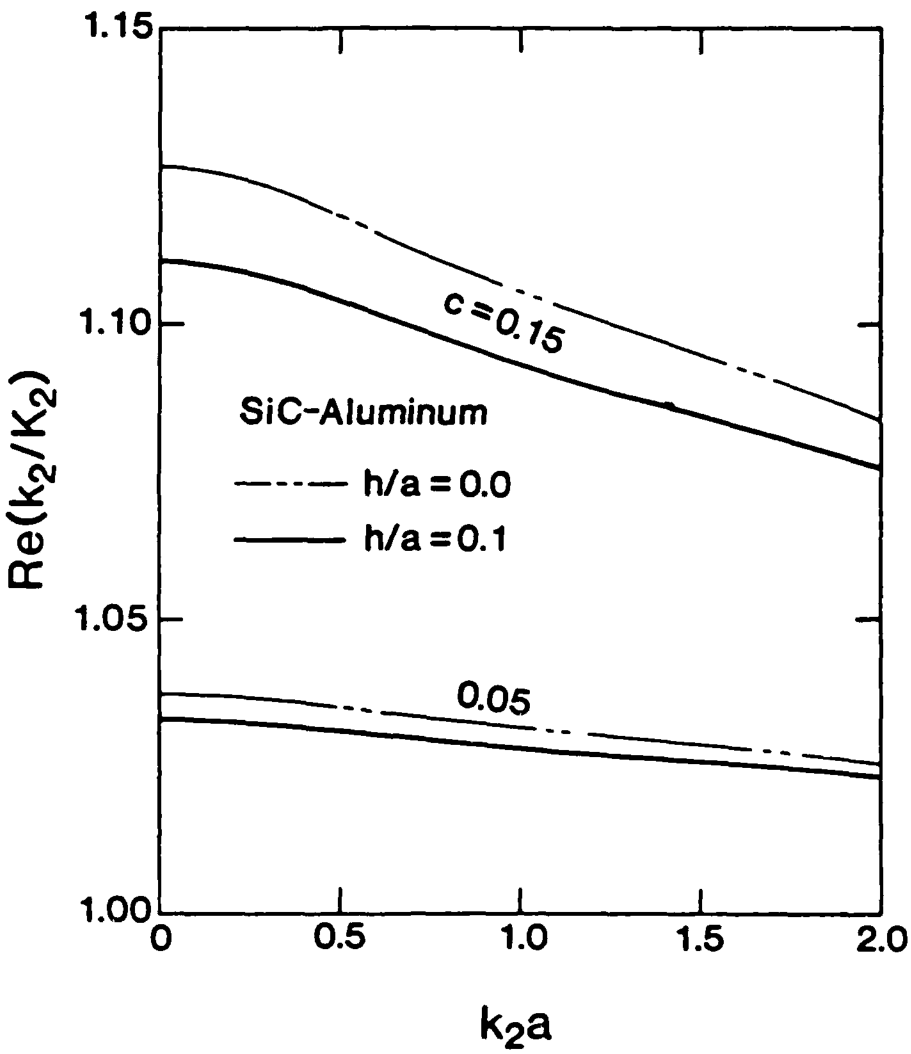
1.15
1.10
1.05
1.00
0
0.5
1.0
1.5
2.0
$Re(k_2/K_2)$
k_2a
c = 0.15
0.05
SiC-Aluminum
h/a = 0.0
h/a = 0.1

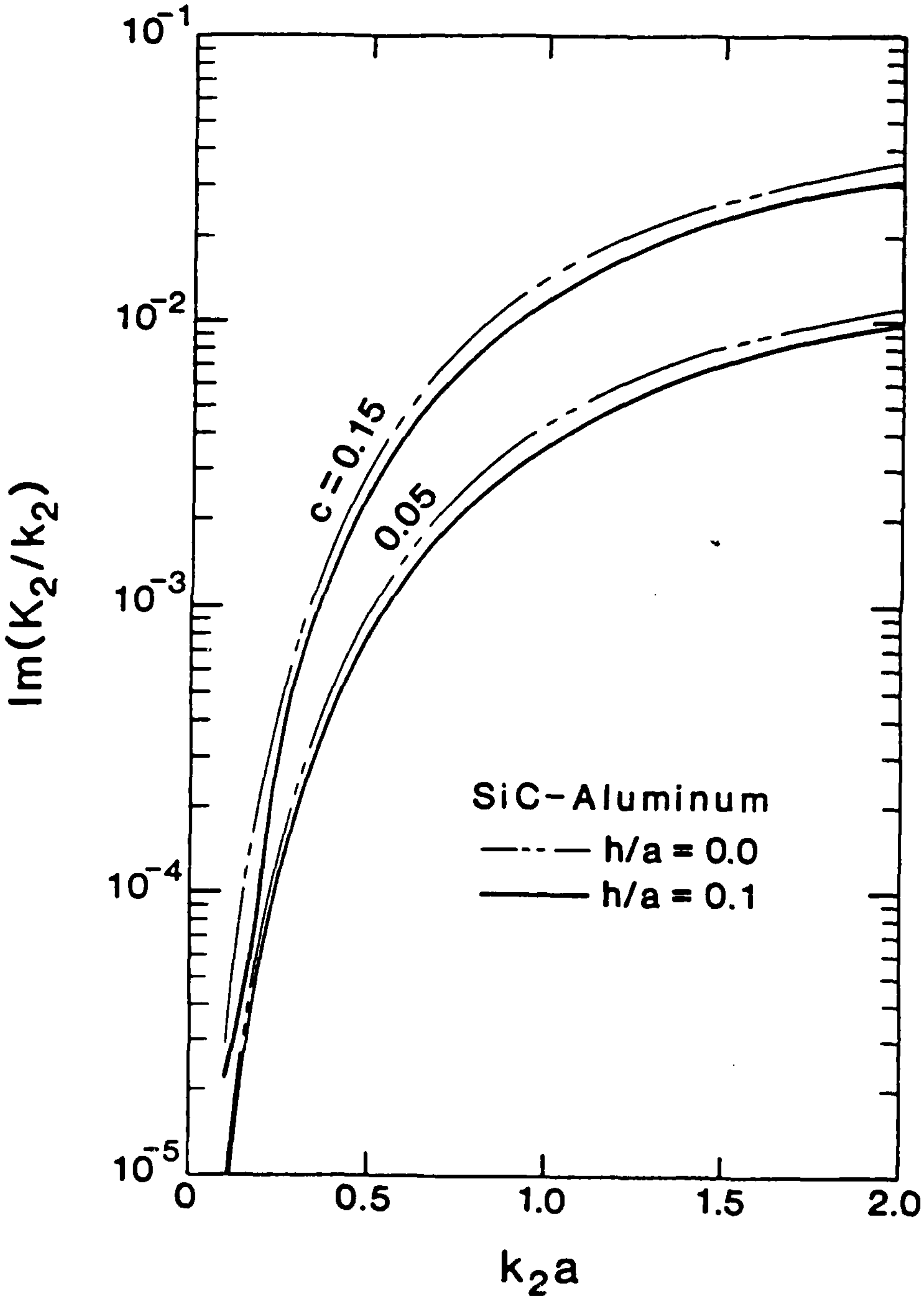

10^-1
10^-2
10^-3
10^-4
10^-5
Im(K2/k2)
c = 0.15
0.05
SiC-Aluminum
h/a = 0.0
h/a = 0.1
0
0.5
1.0
1.5
2.0
k2a

END
DATE
FILMED
3-1988
DTIC